Conical diffraction and Bessel beam formation with a high optical quality biaxial crystal

C. F. Phelan, D. P. O'Dwyer, Y. P. Rakovich, J. F. Donegan and J. G. Lunney

School of Physics, Trinity College Dublin, Dublin 2, Ireland.

Abstract: The manipulation of a Gaussian laser beam using conical diffraction in a high optical quality biaxial crystal of $KGd(WO_4)_2$ has been examined in detail with emphasis on the experimental techniques involved and intuitive explanations of the notable features. Two different optical arrangements were used to form the Pogendorff double-ring light pattern in the focal image plane. The formation of both diverging and non-diverging zeroth and first order Bessel beams was investigated. The various intensity distributions and polarization properties were measured and compared with the predictions of well-established theory.

OCIS codes: (260.1440) Birefringence; (260.1180) Crystal optics; (050.1940) Diffraction

References and Links

1. W. R. Hamilton, "Third supplement to an essay on the theory of systems of rays," Transactions of the Royal Irish Academy **17**, 1–144 (1837).
2. H. Lloyd, "On the phenomena presented by light in its passage along the axes of biaxial crystals" Phil. Mag. **1,** 112–120 and 207–210 (1833).
3. L. D. Landau, E. M. Lifshitz, and L. P. Pitaevskii, *Electrodynamics of Continuous Media 2nd Ed* (Pergamon Press 1984) Chap. 11.
4. M. Born, and E. Wolf, *Principles of Optics 7th Ed* (Cambridge University Press 1999) Chap. 15.
5. J. G. Lunney, and D. W. Weaire, "The ins and outs of conical refraction," Europhys. News **37**(3), 26–29 (2006).
6. A. M. Belskii, and A. P. Khapaluyk, "Internal conical refraction of bounded light beams in biaxial crystals," Opt. Spectrosc. **44**, 312–315 (1978).
7. M. V. Berry, "Conical diffraction asymptotics: fine structure of Poggendorff rings and axial spike," J. Opt. A, Pure Appl. Opt. **6**(4), 289–300 (2004).
8. M. V. Berry, and M. R. Jeffrey, "Conical diffraction: Hamilton's diabolical point at the heart of crystal optics," Prog. Opt. **50**, 13–50 (2007).
9. M. V. Berry, M. R. Jeffrey, and J. G. Lunney, "Conical diffraction: Observations and theory," Proc. R. Soc. A **462**(2070), 1629–1642 (2006).
10. M. V. Berry, M. R. Jeffrey, and M. J. Mansuripur, "Orbital and spin angular momentum in conical diffraction," J. Opt. A, Pure Appl. Opt. **7**(11), 685–690 (2005).
11. L. Allen, S. M. Barnett, and M. J. Padgett, Optical angular momentum (Bristol: Institute of physics publishing 2003).
12. J. Durnin, J. J. Miceli, Jr., and J. H. Eberly, "Diffraction-free beams," Phys. Rev. Lett. **58**(15), 1499–1501 (1987).
13. R. M. Hermann, and T. A. Wiggins, "Production and uses of diffraction free beams," J. Opt. Soc. Am. A **8**(6), 932–942 (1991).
14. S. Gröblacher, T. Jennewein, A. Vaziri, G. Weihs, and A. Zeilinger, "Experimental quantum cryptography with qutrits," N. J. Phys. **8**(5), 75 (2006).
15. L. P. Deng, H. Wang, and K. Wang, "Quantum CNOT gates with orbital angular momentum and polarization of a single photon quantum logic," J. Opt. Soc. Am. B **24**(9), 2517–2520 (2007).
16. J. Leach, M. J. Padgett, S. M. Barnett, S. Franke-Arnold, and J. Courtial, "Measuring the orbital angular momentum of a single photon," Phys. Rev. Lett. **88**(25), 257901 (2002).
17. M. C. Pujol, M. Rico, C. Zaldo, R. Solé, V. Nikolov, X. Santos, M. Aguiló, and F. Díaz, "Crystalline structure and optical spectroscopy of Er^{3+}-doped $KGd(WO_4)_2$ single crystals," Appl. Phys. B **68**, 187–197 (1999).

1. Introduction

Internal conical refraction is a striking optical phenomenon which arises when a beam of light is incident along one of the optic axes of a slab of transparent biaxial crystal. The beam propagates as a skewed non-circular hollow cone inside the crystal, and on leaving the crystal

#111743 - $15.00 USD Received 26 May 2009; revised 26 Jun 2009; accepted 29 Jun 2009; published 13 Jul 2009

it refracts into a hollow cylinder of light. Conical refraction was predicted by Hamilton in 1832 [1], and experimentally verified by Lloyd [2], later that year. A geometrical optics description of conical refraction can be found in Ref. 3 and Ref. 4 and a non-technical description is presented in Ref. 5. The full description of conical refraction requires a wave optics approach; this was first done by Belsky and Khapalyuk [6]. They considered the propagation of an electromagnetic wave through a biaxial crystal as a diffraction problem in the paraxial regime. Their result was an integral transformation relating the input and output beams; thus the term conical diffraction arises. The work of Belsky and Khapalyuk was reformulated by Berry [7,8], who treated the effect of propagation through the crystal as a linear operator transforming the state (the transverse field) of a light beam. Berry's main result was a paraxial solution for the optical field which can be numerically evaluated at any plane normal to the propagation direction. It shows that the conically diffracted beam has a narrow double-ring profile in the focal image plane and then diffracts to yield a beam which has a maximum on axis and is described by a superposition of 0th and 1st order diverging Bessel beams with opposite circular polarizations. These calculations were compared with experiment and the agreement was very close [9].

The aim of this paper is to present the main features of conical refraction from an experimental point of view, while minimising the mathematical complexity of the presentation. Particular emphasis is placed on the novel intensity profiles and polarisation properties which can be produced by using conical diffraction of a Gaussian laser beam. These features may find application in optical tweezing experiments where the doughnut-shaped beam with ½ħ net orbital angular momentum [10,11] may be useful. Conical refraction is an efficient method to generate Bessel beams from a Gaussian laser beam It also avoids some of the limitations of other Bessel beam formation techniques, such as the low efficiency of using a ring aperture in combination with a positive lens [12], or the distortion introduced by the slightly rounded cone apex when using an axicon [13]. The ability to manipulate the beam wavefront in combination with polarization switching suggests a of applications, in particular in the fields of quantum cryptography [14], quantum information processing [15], and high density information transfer [16]. The crystals used are of high optical quality and the results obtained provide a further test of the paraxial theory of conical diffraction.

2. Theoretical method

We consider the case of a circularly polarized Gaussian beam incident along the optic axis of a slab of biaxial crystal of thickness l with principal refractive indices $n_1 < n_2 < n_3$. From Ref. 1–4 we know the polarizations and phases of the plane waves which can propagate in a biaxial crystal as well as the refracted ray directions. The semi-angle A of the cone of light inside the crystal is given by:

$$A = \sqrt{(n_3 - n_2)(n_2 - n_1)} \tag{1}$$

and the radius of the cylinder of light emerging from the crystal is: $R_0 = Al$. The paper by Berry [7] provides a theoretical formalism to sum the contributions of the waves excited by a laser beam in the crystal for a range of directions close to the optic axis. Mathematically, this paraxial solution is a two dimensional vector field related to the incident field by an integral transformation. It can be expressed in terms of the cylindrical polar co-ordinates $\{r, \theta, z\}$, as shown in Fig. 1. For a left-circularly polarized incident Gaussian beam the x- and y-components of the field are given by:

#111743 - $15.00 USD Received 26 May 2009; revised 26 Jun 2009; accepted 29 Jun 2009; published 13 Jul 2009

$$E_x \propto \exp(-\tfrac{r^2}{w^2})$$
$$E_y \propto i\exp(-\tfrac{r^2}{w^2}) \tag{2}$$

In the definition of the Gaussian beam the value of w used here is $\sqrt{2}$ times the value used by Berry. On passing through the biaxial crystal the Gaussian beam is transformed into a beam with field components given by:

$$E_x(r,\varphi,z) \propto B_0(r,z) + B_1(r,z)(\cos\varphi + i\sin\varphi)$$
$$E_y(r,\varphi,z) \propto iB_0(r,z) + B_1(r,z)(\sin\varphi - i\cos\varphi) \tag{3}$$

where B_0 and B_1 are the following integrals involving Bessel functions J_0 and J_1.

$$B_0 = k\int_0^\infty p\cos(kpR_0)J_0(kpr)\exp(-\tfrac{1}{4}k^2p^2w^2)\exp(-\tfrac{1}{2}ikp^2Z) \tag{4}$$

$$B_1 = k\int_0^\infty p\sin(kpR_0)J_1(kpr)\exp(-\tfrac{1}{4}k^2p^2w^2)\exp(-\tfrac{1}{2}ikp^2Z) \tag{5}$$

where $kw^2\exp(-\frac{1}{4}w^2k^2p^2)$ is the Fourier spectrum of the incident field with off axis wave vectors $k\vec{p} = k\{p_x, p_y\}$ where k is the wave number of the beam along the optic axis and $p << 1$ for a paraxial beam; $Z = l + (z-l)n_2$ is the longitudinal co-ordinate measured from the position of the beam waist having taken into account the effect that the refraction on entering the crystal will have on the spreading of the beam and z is longitudinal position measured from the position at which the beam waist would occur if there were no crystal. The sharpest rings are obtained when a second lens is used to image the plane at $Z = 0$, the so-called focal image plane. It is the plane perpendicular to the beam propagation direction in which the virtual image of the waist of the incident beam would appear to be if the beam were incident on an isotropic crystal with refractive index n_2 i.e. the plane at which Z = 0 . The B_0 field component has the same left-circular polarization as the input, while the B_1 component has right-circular polarization but with a 2π azimuthal phase change, this property is explored in more detail in Section 4.

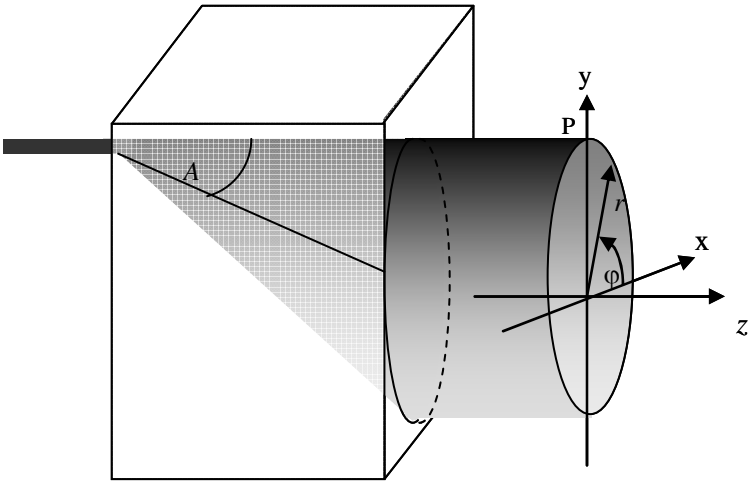

Fig. 1. The system of cylindrical co-ordinates used to describe the cylinder of light that propagates in space after having been refracted into a cone of semi-angle A within the crystal.

#111743 - $15.00 USD Received 26 May 2009; revised 26 Jun 2009; accepted 29 Jun 2009; published 13 Jul 2009

Using Eq. (4) and Eq. (5) we have calculated the free space evolution of a 632 nm wavelength Gaussian beam with w = 25μm from the position of its waist to the far field after propagation through a 3 cm slab of $KGd(WO_4)_2$ crystal whose principal refractive indices are n_1 = 2.013, n_2 = 2.045, n_3 = 2.086, measured by Pujol et al [17]. Figure 2(a) and 2(b) show the calculated intensity distributions in the x-z (or y-z) plane for the B_0 and B_1 components respectively, and Fig. 2(c) shows the intensity distribution due to the sum of these two fields. Near the focal image plane (Z = 0) both the B_0 and B_1 beams comprise two closely spaced rings, where the outer ring is more intense. As the beams propagate beyond the focal image plane they diffract giving rise to a conical superposition of wave fronts. In the focal image plane the separation of the rings is ~1.6ω. Beyond the Rayleigh range, the angle of divergence between the rings is ~4/$k\omega$.

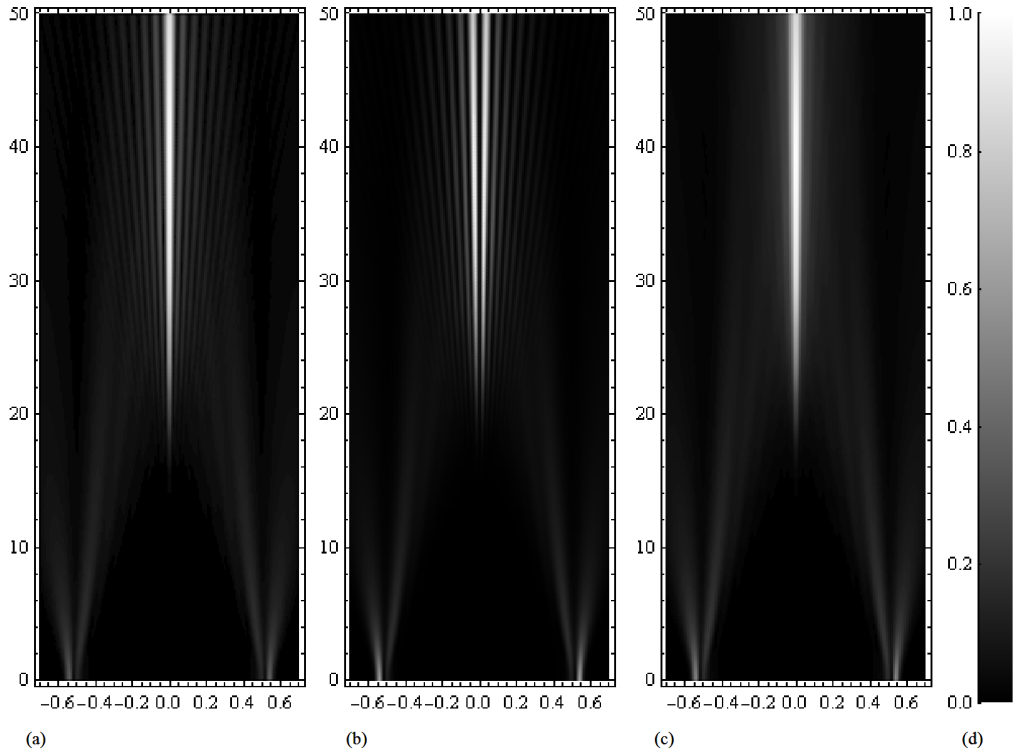

Fig. 2. The intensity due to B_0 (a), B_1 (b) and the conically diffracted Gaussian field, $B_0 + B_1$ (c) as the beam propagates away from the focal image. The vertical axis measures distance from the focal image plane in mm and the horizontal axis measures radial distance in mm. (d) shows the normalized greyscale.

It is of interest to consider the diffraction of the B_0 and B_1 components separately. Taking the Fourier transforms of the distributions in the focal image plane due to B_0 and B_1 (Eq. (4) & Eq. (5)) separately suggests that the far field pattern of the beam should resemble a superposition of zeroth and first order diverging Bessel beams. The B_0 component, which is a double ring of azimuthally uniform amplitude and phase yields a 0th order Bessel beam in the far-field, as shown in Fig. 2(a). However, due to azimuthal variation of phase in the B_1 component, it yields a 1st order Bessel beam, which has zero intensity on axis, as shown in Fig. 2(b). In the experimental measurements presented below we mainly concentrate on the beam profiles in the focal image plane and in the far-field.

#111743 - $15.00 USD Received 26 May 2009; revised 26 Jun 2009; accepted 29 Jun 2009; published 13 Jul 2009

3. Experimental methods

The first optical arrangement used to examine the various beams which can be produced by conical refraction is shown in Fig. 3. The Gaussian beam output of a 10 mW 632 nm He-Ne laser was left–circularly polarized using a linear polarizer and a λ/4 plate. The beam was focused with a x10 microscope objective to form a beam waist radius ω = 14 μm at the $1/e^2$ point. The biaxial crystal used was a 3cm thick slab of $KGd(WO_4)_2$ obtained from *CROptics* [www.croptics.eu] with the same principal refractive indices at 632 nm as used in the calculation in Section 2. The crystal was cut with one of the optic axes perpendicular to the slab faces. In the first setup the incident beam waist was positioned near the input face of the crystal. The output beam was imaged at 1:1 magnification using a 10 cm focal length lens on to a Firewire CCD camera (Thorlabs DC310). Different planes were recorded by moving the imaging lens and CCD camera together.

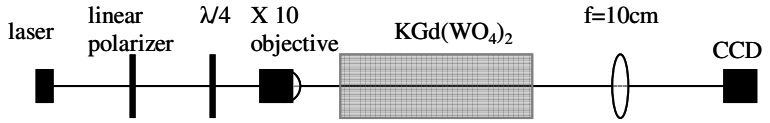

Fig. 3. Circularly polarized light is focused into the crystal with a x10 objective to achieve a narrow waist (10μm). The focal image plane which for this setup occurs somewhere near the crystals entrance face (due to the short focal length of the objective) is imaged onto the CCD with a 10cm focal length lens.

4. Beam properties in focal image plane

The focal image plane intensity profile is shown in Fig. 4. Since the beam waist is near the input face of a 3 cm thick crystal this plane is located at 1.53 cm inside that face. The radius of the dark ring in the focal image plane is found to be 0.53 mm, in close agreement with the expected value of R_0 for A = 0.0177 rad. The separation of the rings is 19μm, which is close to the expected value of 16μm.

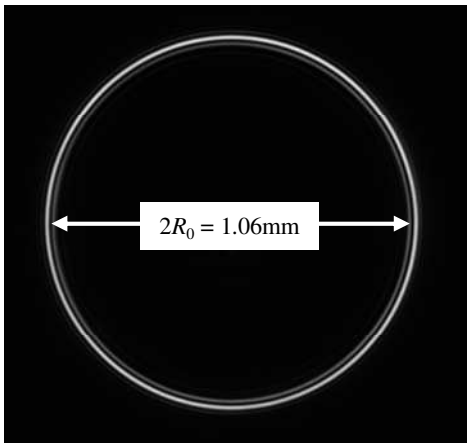

Fig. 4. Experimental image of the focal image plane, the excellent quality of the crystal is obvious from the image above

As is well known, at any point on the focal image plane the polarization is linear but it rotates from tangential at the point on the ring corresponding to the straight-through position (position P in Fig. 1 and 5(a)) to radial at the diametrically opposed point. In fact for all diametrically opposed positions the polarizations are orthogonal. This feature can be readily understood by considering the superposition of the B_0 and B_1 field components in the focal image plane. In Fig. 5(a) we present schematic representation of the addition of these fields.

#111743 - $15.00 USD Received 26 May 2009; revised 26 Jun 2009; accepted 29 Jun 2009; published 13 Jul 2009

The first two rows in that figure show the orientation of the field vector at four successive times differing by quarter of an optical cycle for the B_0 (top) and B_1 (middle) fields. The bottom row shows the coherent addition of these two fields. At any time during the optical cycle the electric field of the B_0 component has the same direction around the ring, while for the B_1 component the field rotates by 2π on moving round the ring. This way of looking at the conically diffracted field gives an intuitively appealing way of understanding the azimuthal variation of polarization. It also provides an insight into the optical angular momentum changes occurring in conical diffraction. The B_0 field is left circular and thus has same spin optical momentum as the input. The B_1 field is right-circular but with an azimuthal phase change of 2π. Thus this field carries spin moment of opposite to the input and orbital momentum of the same sense as the input. The net result is that the while the input beam carries $\hbar$ spin angular momentum per photon, the output beam (sum of B_0 and B_1) carries $\frac{1}{2}\hbar$ orbital angular momentum per photon since B_1 carries half of the input power [14,15]. By using an appropriate circular polarizer we can select either of the two beam components. It should also be noted that the inner and outer rings have opposite phase. This can be seen in Fig. 5(b) which shows a calculation of the radial distribution of the B_0 and B_1 electric field components for the point in the optical cycle corresponding to leftmost panels in Fig. 5(a).

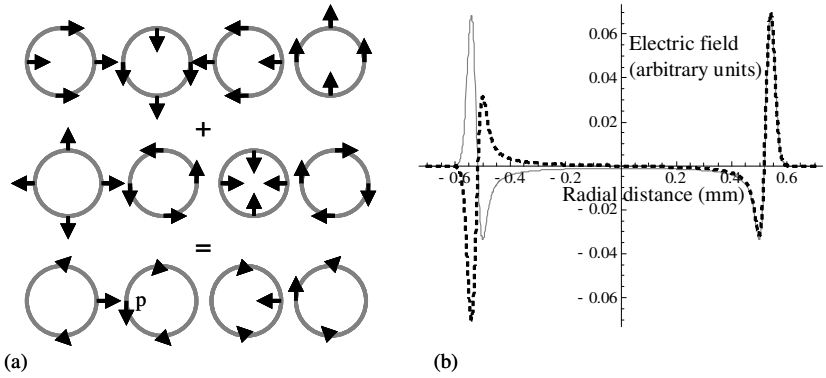

Fig. 5. The different phase properties of the fields described by B_0 & B_1. 5(a) shows, over one optical cycle, the how field vectors of the B_0 component combine with the field vectors of the B_1 field to give the half turn of polarization associated with conical refraction; 5(b)shows a snapshot of the B_0 and B_1 electric field profiles in the focal image plane (B_1 dashed)

Conical diffraction can also be realized using the optical arrangement shown in Fig. 6. Here a longer focal length lens is used to form a real focal image plane beyond the crystal. The beam waist of the focused laser beam was 25 μm. The radius of the dark ring in the transverse plane, which is determined by the length of the crystal, will be the same as before, but the width of the rings, which is dependent on the beam waist at focus, is now larger than before. Figure 7 shows a comparison of the calculated and measured radial intensity distributions in the focal image plane. There is good agreement, showing that the paraxial theory provides a good description of the phenomenon.

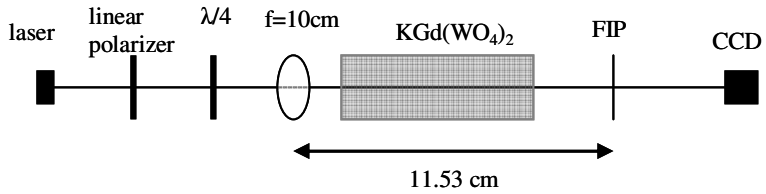

Fig. 6. This optical arrangement used to analyze conical diffraction requires no imaging lens

#111743 - $15.00 USD Received 26 May 2009; revised 26 Jun 2009; accepted 29 Jun 2009; published 13 Jul 2009

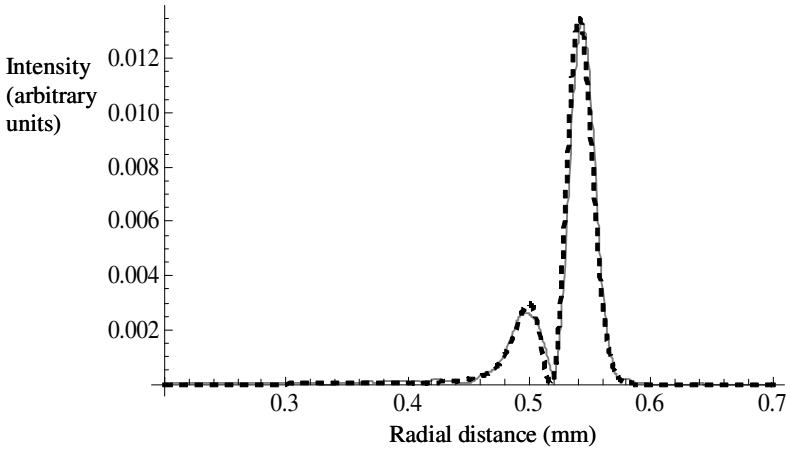

Fig. 7. A comparison of experiment with theory (dashed line) in the focal image plane; Radial distance is measured from the centre of the cylinder associated with conical refraction (Fig. 1)

5. Beam properties in far-field

Figure 8(a) and 8(b) shows the far-field intensity distributions of the B_0 and B_1 beams recorded using the CCD camera placed at 10.75 cm (Z = 22) from the focal image plane. The measured radial intensity distributions are compared with theory in Fig. 9(a) and 9(b), where the agreement of the experiment is seen to be very close, these profiles were obtained using the method outlined in Fig. 6 with the incident beam having a waist of 25μm.

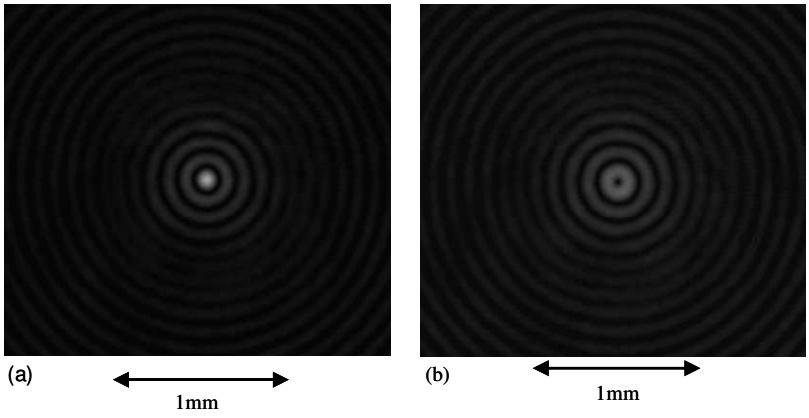

Fig. 8. CCD pictures of diverging Bessel beams; B_0 in (a); B_1 in (b)

#111743 - $15.00 USD Received 26 May 2009; revised 26 Jun 2009; accepted 29 Jun 2009; published 13 Jul 2009

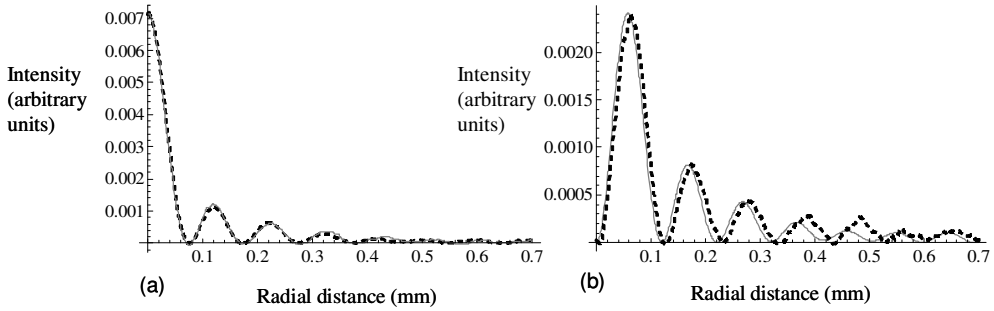

Fig. 9. (a) Exact far field B_0 vs experimental data (dashed) at 10.75 cm from FIP; (b) same data for B_1

The Bessel beams formed by propagation in free space of the focal image plane distribution are divergent. It is possible to use conical diffraction to form non-divergent Bessel beams by using the optical setup shown in Fig. 10. A converging lens is placed at a distance equal to the focal length beyond the focal image plane. Durnin [12] formed the conical superposition of wavefronts required for Bessel beam formation by placing a lens of focal length f at a distance f from a uniformly illuminated ring aperture thus causing the non-diverging Bessel profile to appear in the focal region of the lens. In order to reproduce this situation with our crystal a beam with a larger than usual waist is passed along the optic axis and then brought to a focus by a shorter focal length lens to create a conical superposition of wavefronts. The beam entering the crystal after propagation through a 30cm lens has a waist that was measured to be 234μm. The dark ring that separates the two bright rings in the focal image plane corresponds to a geometrical ray along the optic axis and therefore we expect this to be focused onto the axis at the focal point of the lens with an intensity peak on either side of it. We calculated the positions of these peaks by realizing that the angular range of the beam outside its Rayleigh range is $4/kw$ and using geometrical optics to calculate the position at which a ray directed $2/kw$ away from the axis and a ray directed towards the axis and making an angle $2/kw$ with the axis. The calculation gives the peak to peak separation as 7.9mm while experiment gives peak to peak separation of ~7mm.

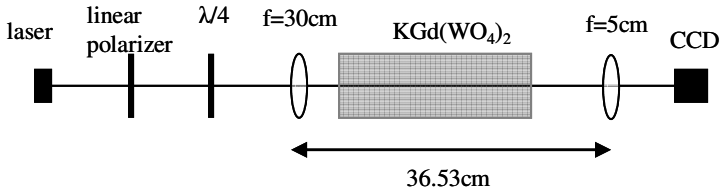

Fig. 10. Optical setup for non-diverging Bessel beams

6. Conclusion

A detailed experimental investigation of conical diffraction in a high optical quality biaxial crystal has been done. Primarily, the aim was to present the main features conical diffraction from an experimental point of view. However, the experimental measurements have been compared with the predictions of well-established theory. Two optical arrangements were used to form the well-known Pogendorff double-ring light pattern in the focal image plane. The propagation of the conically diffracted beam beyond the focal image plane to form diverging zeroth and first order Bessel beams was investigated. Finally, the formation of non-diverging Bessel beams using conical refraction was considered.

#111743 - $15.00 USD Received 26 May 2009; revised 26 Jun 2009; accepted 29 Jun 2009; published 13 Jul 2009

Acknowledgements

This work was supported by Science Foundation Ireland under the Research Frontiers Programme.

#111743 - $15.00 USD Received 26 May 2009; revised 26 Jun 2009; accepted 29 Jun 2009; published 13 Jul 2009